Dicopper(I) Complexes containing Intramolecular 1,2-Diaza Bridging Ligands. Behaviour of the Dicopper Site in the Dehydrogenation of Hydrazobenzene. Crystal Structure of $[Cu_2L^2(pydz)_2][ClO_4]_2$†

Michael G. B. Drew* and Paul C. Yates
Department of Chemistry, The University, Whiteknights, Reading RG6 2AD
Jadwiga Trocha-Grimshaw, Aidan Lavery, Kieran P. McKillop, and S. Martin Nelson
Department of Chemistry, Queens University, Belfast BT9 5AG
(in part) Jane Nelson*
The Open University, Milton Keynes MK7 6AA

Dicopper(I) complexes of two 20-membered N_4 macrocycles and incorporating exogenous 1,2-diaza bridging ligands have been prepared. An *X*-ray crystallographic structure determination of the complex $[Cu_2L^2(pydz)_2][ClO_4]_2$ (pydz = pyridazine, L^2 = 5,5,16,16-tetramethyl-23,24-dioxa-3,7,14,18-tetra-azatricyclo[18.2.1.1^{9,12}]tetracosa-2,7,9,11,13,18,20,22-octaene) has been carried out. Crystals are monoclinic, space group $P2_1/c$ with $a = 9.71(1)$, $b = 15.64(2)$, $c = 12.52(1)$ Å, $\beta = 105.5(1)°$, and $Z = 2$. In the centrosymmetric cation the copper atoms have a distorted tetrahedral environment, being bonded to two nitrogens of the macrocycle [2.010(13), 2.044(11) Å] and to the nitrogen atoms of the bridging pydz molecules [1.938(14), 2.116(14) Å]. The Cu ··· Cu distance is 3.150(5) Å. Dicopper complexes of L^2 catalyse the dehydrogenation of hydrazobenzene to *trans*-azobenzene in cleaner and more quantitative fashion but at a slower rate than free Cu^I ions.

The binucleating macrocycle L^1 shows a particular facility for adopting single-atom bridges. Because of its size, the macrocycle cannot accommodate the normal three-atom -NCS- bridge where the metal atoms need to be *ca.* 5.5 Å apart. Instead it adopts the rare nitrogen-atom only[1] or sulphur-atom only[2] bridging mode, where the metal atoms are *ca.* 3.0 Å apart, a distance much more compatible with low-energy conformations of the macrocycle. The hydroxo and alkoxo single oxygen-atom bridges are also favoured in this macrocyclic system especially with dicopper(II) complexes. The prevalence of the single-atom bridge suggested the possibility that a *O*-peroxo-bridged adduct might be the active species in oxidations catalysed[3] by dicopper complexes of L^1. The *O,O'*-peroxo-species, more usually postulated as active species in copper-catalysed oxidations, requires a two-atom bridge between copper centres, which may be unfavourable in L^1 dicopper complexes. In order to see whether a two-atom bridge can be accommodated between copper centres, we attempted the synthesis of dicopper complexes of this macrocycle incorporating one or more exogenous 1,2-diaza bridges.

Results and Discussion

The ligands L^1 and L^2 used in the present study were synthesised by template Schiff-base condensation of 2,5-diformylfuran with the appropriate diamine on Group 2 metal ions M^{2+}. On treatment of the appropriate $[ML]^{2+}$ salt ($L = L^1$ or L^2) with $Cu(ClO_4)_2$ in ethanol, the product is the di-μ-hydroxo complex $[Cu_2L(OH)_2][ClO_4]_2 \cdot H_2O$; when transmetallation is carried out using $[Cu(MeCN)_4]ClO_4$, the dicopper(I) complexes $[Cu_2L(MeCN)_2][ClO_4]_2$ are obtained. As noted earlier,[3] both complexes display catalytic activity in the dehydrogenation of a range of substrates containing labile hydrogen. When the dicopper(I) complexes were treated with excess of the 1,2-diaza donors pyridazine or *cis*-azobenzene, the products described below were obtained.

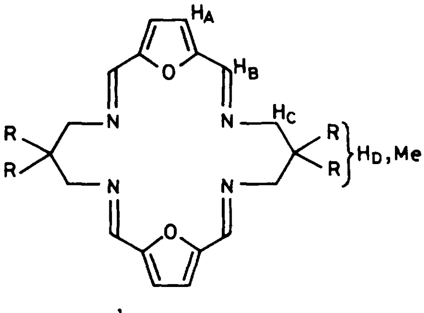

L^1 ; R = H
L^2 ; R = Me

On the addition of pyridazine (pydz), compounds analysing to $[Cu_2L(pydz)_2][ClO_4]_2$ ($L = L^1$ or L^2) crystallized out (Table 1). These are 1:2 electrolytes which i.r. spectra show to contain the intact macrocycle and ionic perchlorate. In the electronic spectrum, a poorly resolved shoulder on the low-frequency side of the main ligand absorption can be assigned to a d-π^* metal to ligand charge-transfer (m.l.c.t.) transition of the Cu^I-pydz chromophore. An *X*-ray crystallographic structure determination, carried out on the L^2 complex $[Cu_2L^2(pydz)_2][ClO_4]_2$, indicates that co-ordination of the pair of two-atom bridges, one above and one below the macrocyclic plane, is accompanied by some unusual geometry in the substrate molecule, suggesting steric constraints. However, the ^1H n.m.r. spectrum of the substrate displays only small co-ordination shifts, the major change observed being in the α-proton signal which shifts upfield (Table 2) by 0.15—0.25 p.p.m., reflecting alteration of ring current on co-ordination due presumably to a combination of geometric and electronic factors.

---

† Di-μ-[pyridazine-*N*(Cu),*N'*(Cu')]-{5,5,16,16-tetramethyl-23,24-dioxa-3,7,14,18-tetra-azatricyclo[18.2.1.1^{9,12}]tetracosa-2,7,9,11,13,18,-20,22-octaene-*NN'*(Cu):*N''N'''*(Cu')}dicopper(I) bis(perchlorate).

Supplementary data available: see Instructions for Authors, *J. Chem. Soc., Dalton Trans.*, 1988, Issue 1, pp. xvii—xx.

Table 1. Physical data

Complex	Colour	Analysis[a] (%) N	C	H	Λ^b/S cm^2 mol^{-1}	Infrared data/cm^{-1} ν(C–H)		ν(C=N)	$\nu_3(ClO_4^-)$	$\nu_4(ClO_4^-)$	Electronic spectra $\lambda_{max.}$/cm^{-1}	ε/dm^3 mol^{-1} cm^{-1}
$[CaL^2][ClO_4]_2$	Colourless	8.8 (9.0)	42.3 (42.7)	4.7 (4.6)	328	3 100	2 950 2 920 2 855	1 628 1 618	1 115 1 150	620 628	33 800	42 000
$[Cu_2L^2(MeCN)_2]$-$[ClO_4]_2$	Yellow	10.7 (10.7)	39.8 (39.6)	4.3 (4.3)	275	3 120	2 940— 2 980	1 625	1 085	622	34 000	39 380
$[Cu_2L^1(MeCN)_2]$-$[ClO_4]_2$	Yellow	11.7 (11.5)	35.8 (36.1)	3.8 (3.6)	262	3 120 3 080	2 940— 2 840	1 624	1 085	621	34 900	40 300
$[Cu_2L^1(OH)_2][ClO_4]_2\cdot H_2O$	Green	11.8 (11.0)	34.9 (34.7)	3.7 (3.9)	252	3 120 3 100	2 950— 2 840	1 640	1 090	623	34 860 15 100	31 380 140
$[Cu_2L^1(pydz)_2]$-$[ClO_4]_2\cdot MeCN$	Red-brown	14.7 (14.8)	39.6 (39.4)	3.6 (3.7)	245	3 120 3 080	2 980— 2 900	1 620 1 610	1 090	621	35 000 26 000br (sh)	45 000
$[Cu_2L^2(pydz)_2]$-$[ClO_4]_2$	Red-brown	12.9 (12.9)	41.6 (41.6)	3.9 (4.2)	250	3 120 3 085	2 980— 2 850	1 620 1 610	1 090	621	34 700 25 000br (sh)	50 000
$[Cu_2L^1(cis\text{-}Ph_2N_2)_2]$-$[ClO_4]_2$	Very dark red	10.9 (11.0)	49.9 (49.7)	4.0 (4.0)	251	3 120— 3 040	2 920— 2 820	1 624	1 090	620	34 500 23 800	49 000 2 700
$[Cu_2L^2(cis\text{-}Ph_2N_2)$-$(MeCN)][ClO_4]_2$	Very dark red	10.5 (10.5)	46.2 (46.5)	4.5 (4.4)	285	3 120 3 080 3 047	2 950 2 820 2 860	1 632	1 085	621	34 700 23 500	53 800 2 000

[a] Calculated values in parentheses. [b] 10^{-3} mol dm^{-3} solutions in MeCN.

Table 2. ^{1}H N.m.r. data[a] (δ/p.p.m. from $SiMe_4$)

Complex	H_A	H_B	H_C	H_D or Me_D				
$[BaL^1][ClO_4]_2$	7.10 (s)	8.22 (s)	3.90 (br)	1.90 (br)				
$[CaL^2][ClO_4]_2$	7.09 (s)	8.26 (s)	3.48 (s)	1.00 (s)				
$[Cu_2L^1(MeCN)_2][ClO_4]_2$	7.20 (s)	8.25 (s)	3.99 (t)	*b*				
$[Cu_2L^2(MeCN)_2][ClO_4]_2$	7.25 (s)	8.23 (s)	3.81 (s)	1.01 (s)				
					m	*p*	*o*	
cis-Ph_2N_2					7.28 (m)	7.16 (m)	6.83 (m)	
					m + *p*		*o*	
trans-Ph_2N_2					7.56 (m)		7.94 (m)	
Hydrazobenzene					7.16 (m)		6.81 (m)	6.37 (br,s)[c]
$[Cu_2L^1(Ph_2N_2)_2][ClO_4]_2$	7.30 (s)	8.25 (s)	3.85 (t)	1.84 (m)	7.25 (m)		6.74 (m)	
$[Cu_2L^2(Ph_2N_2)(MeCN)][ClO_4]_2$	*b*	8.18 (s)	3.70 (br,s)	0.95 (s)	7.25 (m)		6.87 (m)	
					α		β	
Pyridazine					9.18 (t)		7.58 (q)	
$[Cu_2L^1(pydz)_2][ClO_4]_2$	7.03 (s)	8.13 (s)	4.12 (t)	*b*	8.92 (t)		7.69 (q)	
$[Cu_2L^2(pydz)_2][ClO_4]_2$	7.17 (s)	8.16 (s)	3.95 (s)	1.0 (s)	9.03 (br)		7.71 (br)	

[a] All spectra in CD_3CN. [b] Obscured by other signals. [c] NH protons.

From reaction with *cis*-azobenzene, the compounds $[Cu_2L^1(Ph_2N_2)_2][ClO_4]_2$ and $[Cu_2L^2(Ph_2N_2)(MeCN)][ClO_4]_2$ were obtained as very dark red crystalline solids. Conductivity measurements and i.r. spectra show that the perchlorates are unco-ordinated in these complexes, indicating four-co-ordination for Cu^I in $[Cu_2L^1(Ph_2N_2)_2][ClO_4]_2$. In $[Cu_2L^2(Ph_2N_2)(MeCN)][ClO_4]_2$, one Cu^I ion is apparently three-co-ordinate. Failure to isolate a di-μ-azobenzene derivative with the more hindered macrocycle L^2 suggests that steric interactions are more severe with the *cis*-azobenzene bridge than with pyridazine. However, it seems that these are not so severe as to force the macrocycle to adopt the folded conformation which manifests itself[4] in the ^{1}H n.m.r. spectrum by further splitting of the methylene signals. There is no additional splitting of methylene signals, even in the di-μ-azobenzene derivative, which suggests a basically planar macrocyclic conformation, with Cu^I occupying a tetrahedral site made up of two imino nitrogens and the two proximal aza nitrogens from the pair of azobenzene bridges lying above and below the macrocyclic plane.

The ^{1}H n.m.r. spectrum of *cis*-azobenzene (Table 2) is barely affected by co-ordination, the most noticeable effect being that the *para*-proton signal is no longer resolved from the *meta* signal, due, no doubt, to minor changes in long-range shielding by the *cis*-disposed aromatic rings. The macrocyclic spectrum is in general unaffected by bridge formation, the furan protons being the most sensitive to co-ordination effects. Thus, in comparing the chemical shift in $[BaL^1]^{2+}$ where the furan oxygen is co-ordinated, with that in $[Cu_2L^1(MeCN)_2]^{2+}$ where it is unco-ordinated, a downfield shift of 0.19 p.p.m. is observed. Where *cis*-azobenzene is co-ordinated to the copper centres, a further small downfield shift of 0.1 p.p.m. is observed, but an upfield shift of 0.17 p.p.m. results from the di-co-ordination of pyridazine. Presumably these small shifts are a consequence of

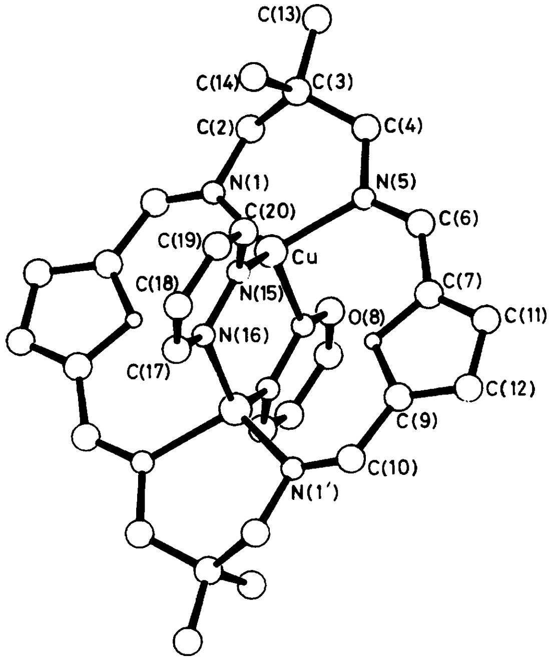

Figure 1. Structure of the $[Cu_2L^2(pydz)_2]^{2+}$ cation showing the atomic numbering scheme

the additional ring currents generated by the aromatic substrates which are held at different distances from, and in different orientations relative to, the furan protons.

The azobenzene complexes, which owe their intense colour to a broad $Cu^Id \longrightarrow \pi^*$ m.l.c.t. band occurring in the visible region, are relatively air stable. In contrast to the unbridged dicopper(I) complexes $[Cu_2L(MeCN)_2]^{2+}$, they oxidise only slowly over a period of days to give green Cu^{II}-containing solutions. The pyridazine-bridged complexes are likewise stabilised towards oxidation by the additional delocalisation in the co-ordination sphere; so much so that the dicopper(I) complex may be obtained from dicopper(II) starting materials merely by addition of pyridazine.

The preparation of these 1,2-diaza-bridged complexes, and the crystal structure which follows, show that the Cu^I–N–N–Cu^I unit may be accommodated in both L^1 and L^2 macrocycles although apparently with some strain in the bridge. The same is true of dicopper(II) complexes of these macrocycles. The crystal structure of a di-μ-pyrazolyl-bridged L^1 complex[4] shows that a two-atom bridge can exist between dicopper(II) sites, although in this structure it is accompanied by folding of the macrocycle into a saddle shape, both bridges being disposed to the same side.

X-Ray Crystallographic Structure Determination of $[Cu_2L^2(pydz)_2][ClO_4]_2$ (**1**).—The structure of $[Cu_2L^2(pydz)_2][ClO_4]_2$ (**1**) is shown in Figure 1 together with the atomic numbering scheme. The two copper atoms are bridged by two pyridazine molecules with a Cu $\cdots$ Cu distance of 3.150(5) Å.

The copper atoms are four-co-ordinate with a distorted tetrahedral environment being bonded to a nitrogen atom [2.116(14), 1.938(14) Å] in each of the bridging ligands together with two nitrogen atoms of the macrocycle [2.010(13), 2.044(11) Å].

The angle between these two CuN_2 planes is 79.5° compared to the expected value of 90° for a tetrahedron. The Cu atoms are not bonded to the furan oxygen atoms (Cu–O > 2.90 Å).

The conformation of the macrocycle can be analysed *via* least-squares planes. The four nitrogen donor atoms in the macrocycle are perforce coplanar and the copper atoms lie on opposite sides of this plane at distances of ± 0.18 Å. The furan and pyridazine rings are each planar to within experimental error and intersect at angles of 72.5°. The furan rings are almost planar with the N_4 plane, intersecting it at angles of 6.5°. Most of the torsion angles within the macrocycle are close to their ideal values indicating a low degree of strain. However, there are deviations of *ca.* 15° around C(2)–C(3) and C(4)–N(5) from the ideal values of 60 and 180° respectively; the greatest twist is across N(1)–C(2) where the torsion angle is $-144°$ which is 24° from its ideal value.

A search of the Cambridge Crystallographic Data Centre files for pyridazine structures located several substituted pyridazines with Cu^{II} but only one structure containing Cu^I, *viz.* $[\{Cu(CN)(pydz)\}_n]$ (**2**).[5] This complex is polymeric and contains bridging cyanide ligands as well as bridging pyridazine ligands but within it is a $Cu_2(pydz)_2$ bridge moiety in which the two copper atoms, which have distorted tetrahedral environments, are situated on a crystallographic mirror plane. The Cu $\cdots$ Cu distance is 3.68 Å, the Cu–N–N–Cu torsion angles are +39.8 and −39.8°, and the two rings intersect each other at 20.2°. This compares with dimensions of 3.15 Å, +25.5, −25.5, and 0.0° in (**1**).

It seems likely that the reason for the difference in bridge dimensions in the two structures is the different steric constraints of the polymer in (**2**) and the macrocycle in (**1**).

Particularly noticeable are the N–Cu–N angles within the bridges which are close to the expected tetrahedral values in (**2**) (105.3, 109.4°) but very much larger in (**1**) [126.0(5)°]. This suggests that the more normal Cu $\cdots$ Cu distance for this type of bridge is *ca.* 3.65 Å and that the much closer distance in (**1**) is caused by the steric constraint of the macrocycle. Molecular mechanics calculations[6] show a preferred Cu $\cdots$ Cu distance of *ca.* 3.0 Å in a variety of L^1 complexes, considerably less than the values found in the polymeric (**2**).

The dimensions of the pyridazine ligands in (**1**) are unusual in that C(17)–C(18) and N(15)–C(20) are particularly short. This could well be a consequence of the different Cu–N distances; Cu–N(16′) at 1.938(14) Å is significantly shorter than Cu–N(15) at 2.116(14) Å. This difference might well lead to the asymmetry of the bridging ligand, with the N(15)–C(20) bond showing more double-bond character than N(16)–C(17). It is perhaps relevant that in (**2**), the Cu–C and Cu–N (copper to cyanide) bond lengths are 1.92(1) and 1.96(1) Å,[5] whereas the Cu–N (macrocycle) distances in (**1**) are 2.010(13) and 2.044(11) Å, thus indicating that the metal atom is able to form stronger Cu–N(pyridazine) bonds in (**1**) than in (**2**).

Even so it is surprising that N(15)–N(16) is 1.400(17) Å by comparison with 1.34(1) Å in (**2**) although the difference may not be significant in view of the standard deviations. Indeed the N–N distances in all the bridging pyridazine structures with Cu^I or Cu^{II} in the Cambridge Crystallographic Data Centre files range from 1.25 to 1.38 Å with a mean of 1.34 Å. It is interesting that in all the copper(II) structures the Cu–N–N–Cu torsion angles are less than 10°, whereas both the copper(I) structures (**1**) and (**2**) have Cu–N–N–Cu torsion angles of ± 25.5 and $\pm 39.8°$ respectively.

The perchlorate anion is ordered and neither ion is involved in any intermolecular contacts less than the sum of the van der Waals radii.

Catalytic Dehydrogenation of Hydrazobenzene; Oxygen Uptake Experiments.—The fact that a stereochemical match (however imperfect) exists between Cu_2L and 1,2-diaza species prompted us to examine the efficacy of dicopper complexes of L^1 as catalysts for the dehydrogenation of hydrazobenzene (1,2-diphenylhydrazine).

Oxygen uptake experiments were performed in *NN*-dimethylacetamide (dma) under one atmosphere of O_2, using $[Cu_2L^1$-

Table 3. Oxygen uptake data in dma for hydrazobenzene dehydrogenation at 30 °C

Catalyst	[Catalyst]/mol dm^{-3}	[PhNHNHPh]/ mol dm^{-3}	Mol O_2/mol PhNHNHPh[a]	Reaction time	
				$t_{\frac{1}{2}}$/min	Complete uptake/min
$[Cu_2L^1(MeCN)_2][ClO_4]_2$	2.41×10^{-3}	4×10^{-2}	0.49	(8)[b]	20
	2.47×10^{-4}	4×10^{-2}	0.60	56	240
$[Cu_2L^1(OH)_2][ClO_4]_2$	2.4×10^{-3}	4×10^{-2}	0.49	(7)[b]	20
	2.5×10^{-4}	4×10^{-2}	0.56	30	180
$Cu(ClO_4)_2{\cdot}6H_2O$	5.19×10^{-4}	4×10^{-2}	0.83	18	68
$Cu(ClO_4)_2{\cdot}6H_2O–OH^-$[c]	5.16×10^{-4}	4×10^{-2}	0.84	15.5	53
$[Cu(MeCN)_4]ClO_4$	2.4×10^{-3}	4×10^{-2}	0.56	(4)[b]	25
	5.1×10^{-4}	4×10^{-2}	0.75	5	43
No catalyst		4×10^{-2}	0.80[d]	372	1 800[d]

[a] All uptakes ±0.03 mol. [b] Rough estimate only possible. [c] 1:1 ratio. [d] Slow uptake continues.

Table 4. Isomeric composition of the products of hydrazobenzene dehydrogenation

Oxidant	Oxidant: PhNHNHPh ratio	Solvent	Azobenzene yield (%)	
			cis	*trans*
$[Cu_2L^1(OH)_2][ClO_4]_2$	1:1	CD_3CN	0	100
$Cu(ClO_4)_2{\cdot}6H_2O$	2:1	CD_3CN	0	77
O_2 alone		CD_3CN	40[a]	60[a]
		CH_3CN	34[b]	66[b]
$[Cu(MeCN)_4]^+–O_2$	2:1	CD_3CN	30[a]	70[a]
	1:20	CH_3CN	28[b]	72[b]
	1:20	dma	12[b]	88[b]
$[Cu_2L^1(MeCN)_2]^{2+}–O_2$	1:1	CD_3CN	0[a]	100[a]
	1:20	dma	0[b]	100[b]

[a] Using ^1H n.m.r. data (±2%). [b] Using u.v. data (±5%).

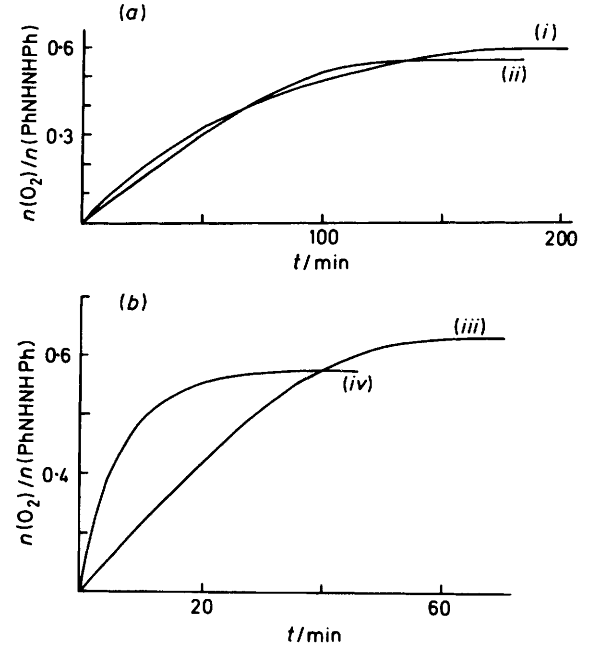

Figure 2. Typical oxygen uptake plots showing the rate of uptake of oxygen per mol of hydrazobenzene (mol ratio *vs.* time) in dma at 30 °C using various catalysts: (*a*) (*i*) $[Cu_2L^1(MeCN)_2][ClO_4]_2$ at 0.006 × substrate concentration, (*ii*) $[Cu_2L^1(OH)_2][ClO_4]_2{\cdot}H_2O$ at 0.006 × substrate concentration; (*b*) (*iii*) $Cu(ClO_4)_2{\cdot}6H_2O$ at 0.003 × substrate concentration, (*iv*) $[Cu(MeCN)_4]ClO_4$ at 0.003 × substrate concentration

$(MeCN)_2][ClO_4]_2$ or $[Cu_2L^1(OH)_2][ClO_4]_2$ as catalysts. The overall stoicheiometry per mol of hydrazobenzene (Table 3), starting with either oxidised or reduced forms of the catalysts, was found to be in the range 0.49—0.60 depending somewhat on catalyst concentration. It seems that at lower catalyst concentrations there is an opportunity for side reactions, leading to products with oxidizable functions (*e.g.* aromatic amines, readily oxidised to nitroso compounds), which could account for O_2 uptakes as high as 0.8 per mol of hydrazobenzene. Such side reactions seem more important when 'free' $Cu(ClO_4)_2$ or $[Cu(MeCN)_4]ClO_4$ is used as catalyst as in these cases the stoicheiometry observed is above 0.5 per mol of hydrazobenzene at all concentrations investigated (Table 3). In the absence of catalyst hydrazobenzene reacts slowly with O_2 taking up 0.80 mol O_2 per mol over a period of 30 h (though a very slow uptake continues after that time).

The rate of uptake of O_2 is compared in Figure 2(*a*) where $[Cu_2L^1(MeCN)_2]^{2+}$ and $[Cu_2L^1(OH)_2]^{2+}$ are used as catalysts with that in Figure 2(*b*) where free Cu^I or Cu^{II} is used. As can be seen, the rate of uptake is faster with 'free' copper ions than the macrocyclic complexes. This suggests that in this system, unlike the 3,5-di-t-butylcatechol dehydrogenation studied earlier,[3,7] no advantage derives from the ready made dicopper site. Indeed, as addition of a stoicheiometric amount of base to $Cu(ClO_4)_2$ barely affects the rate of reaction, it seems that catalysis by 'free' Cu^{II} in this system does not involve even a transient dicopper site.

The function of copper ions as oxidation catalysts involves redox processes where the metal cycles between +1 and +2 oxidation states. For catalysis of dehydrogenation by free copper ions, autoxidation of Cu^I plays a relatively indirect role, and the overall rate is determined by the slower of processes (1) or (2) (X_2H_2 represents a substrate containing labile hydrogen).

$$2\,Cu^{II} + X_2H_2 \longrightarrow 2\,Cu^{I} + X_2 + 2\,H^+ \qquad (1)$$

$$2\,Cu^{I} + 2\,H^+ + 0.5\,O_2 \longrightarrow 2\,Cu^{II} + H_2O \qquad (2)$$

As it is clear[3] that the effect of L^1 co-ordination on copper is a relative stabilisation of the +1 state, it seems likely that process (2) is the one which has been affected in this case. Co-ordination of Cu^I by the macrocyclic ligand appears to have retarded this reaction significantly, perhaps even to the stage where an alternative dehydrogenation mechanism becomes favourable. In an attempt to obtain further information about the difference in the dehydrogenation process when catalysed by 'free' *versus* macrocyclic copper catalysts, we examined the isomeric composition of the azobenzene products produced.

Stereoisomeric composition of the azobenzene product. The oxidation of hydrazobenzene by Cu^{II} in CD_3CN solution was investigated using ^1H n.m.r. spectroscopy (Table 4). At the concentration necessary for n.m.r. observations, and using a stoicheiometric ratio of Cu^{II}:hydrazobenzene, oxidation takes place virtually instantaneously. When $[Cu_2L^1(OH)_2][ClO_4]_2$ is used as oxidant, a quantitative yield of *trans*-azobenzene is obtained. With $Cu(ClO_4)_2$, the only azobenzene obtained is again the *trans* isomer, but the oxidation is not quantitative and *ca.* 33% of another aromatic species (apparently an amine) is seen in the ^1H n.m.r. spectrum. When a CD_3CN solution of hydrazobenzene is allowed to oxidise in air in the absence of catalyst over a period of *ca.* 6 d, both *cis* and *trans* isomers are produced in comparable proportions.

When $[Cu(MeCN)_4]ClO_4$ is used under aerobic conditions, oxidation is somewhat faster than in the absence of Cu^I and results in the formation of a sizeable proportion of the *cis* isomer. On the other hand, when the experiment is carried out using $[Cu_2L^1(MeCN)_2][ClO_4]_2$ in the presence of O_2, a quantitative yield of the *trans* isomer is obtained within 24 h. As the ^1H n.m.r. experiments were carried out in CD_3CN, which is not in general a suitable solvent for O_2 uptake experiments because of its tendency to stabilise the $+1$ oxidation state, the products of hydrazobenzene oxidation, both in MeCN and in dma as solvent, were also examined by electronic spectroscopy (Table 4). Both n–π^* and π–π^* transitions in *cis*- and *trans*-azobenzene are seen at wavelengths too closely similar to be resolvable. However, as the absorption coefficients are markedly different [*cis*-azobenzene (π–π^*): λ 288 nm, ε 7 500 $dm^3\ mol^{-1}\ cm^{-1}$ (dma); *trans*-azobenzene (π–π^*): λ 318 nm, ε 18 000 $dm^3\ mol^{-1}\ cm^{-1}$ (dma)], the absorbance at *ca.* 300 nm can be used to estimate the approximate composition of the isomeric mixture. This approach was used to verify the result of the ^1H n.m.r. experiment that in MeCN solution an appreciable fraction of the *cis* isomer was produced when dehydrogenation was effected by O_2 alone or by O_2 in the presence of $[Cu(MeCN)_4]^+$. In dma solution, analysis of the intensity of the peak at *ca.* 300 nm indicates complete *trans*-azobenzene formation when the macrocyclic dicopper catalyst $[Cu_2L^1(MeCN)_2]^{2+}$ is used, but something more than 10% formation of the *cis* isomer with the mononuclear $[Cu(MeCN)_4]^+$ catalyst.

The clean and quantitative nature of the transformation from hydrazobenzene to *trans*-azobenzene (Table 4) when the macrocyclic catalyst is used, together with the difference in O_2 uptake rate, suggests that a different dehydrogenation mechanism may apply when the macrocyclic dicopper site is used as the catalyst. The stereochemical result suggests that co-ordination of the substrate may be involved. Co-ordination of substrate to the dicopper site requires a mutally *cis* orientation of N lone pairs, which presumably is accompanied by the *anti* arrangement of phenyl groups (shown to be the lowest-energy conformation in the gas phase[8]), see below.

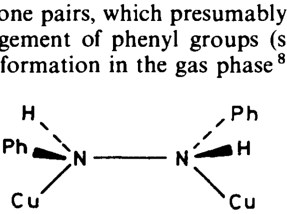

It is easy to see how this geometry leads to the formation of *trans*-azobenzene, even in the limiting case of a one-step concerted dehydrogenation process.

Although (with one exception[9]) previous reports on the catalytic dehydrogenation of hydrazobenzene do not comment on the isomeric composition of the azobenzene product, the predominance of the *trans* isomer is unsurprising given that it is the thermodynamically stable isomer. However, taken together with data on reaction rates, the exclusive formation of the *trans* isomer with the macrocyclic dicopper catalyst is at least consistent with a mechanism which includes co-ordination of hydrazobenzene.

If a cycle similar to that proposed[4] for catechol dehydrogenation applies to hydrazobenzene dehydrogenation at the Cu_2L^1 site, the poorer performance of this catalyst in relation to hydrazobenzene could be rationalised on the basis of steric considerations: (*i*) the difficulty of achieving a Cu_2N_2 plane in the substrate/catalyst adduct owing to steric interactions in the eclipsed substrate conformation which co-ordination necessitates, and (*ii*) the less than perfect match between the dicopper site and hydrazobenzene lone pairs. These are directed outwards from the donor atoms in hydrazobenzene, but in catechol point inwards in chelating fashion, see below.

Co-ordination of an N–N bridge is achieved only at the cost of some strain, as the *X*-ray structure has shown; steric problems are likely to be more severe with hydrazobenzene given the tetrahedral disposition of the phenyl rings.

Taken overall, these factors result in a slower rate of dehydrogenation for hydrazobenzene with Cu_2L^1 than with free copper ions in contrast to catechol dehydrogenation where the reverse is the case. This result, and particularly the implication that the *O,O'*-peroxo bridge may be sterically unfavourable in this macrocycle,[6] provides some indirect evidence against the intermediacy of a *O,O'*-peroxo bridge in the transition state for Cu_2L^1 catalysed oxidations.

Experimental

Complexes of ligand L^1 were prepared by template condensation of 2,5-diformylfuran and 1,3-propanediamine on Group 2 metal ions as described previously.[10] A similar method was used for the preparation of $[CaL^2]^{2+}$. To a suspension of 2,5-diformylfuran (4 mmol) in ethanol (50 cm^3) was added $Ca(ClO_4)_2 \cdot 6H_2O$ (3.6 mmol) and 2,2-dimethylpropane-1,3-diamine (4 mmol). The mixture was stirred at room temperature overnight and the white crystalline product $[CaL^2][ClO_4]_2$, was obtained in 75% yield.

Preparation of the Dicopper Complexes.—$[Cu_2L^1(OH)_2][ClO_4]_2 \cdot H_2O$ To a suspension of $[BaL^1][ClO_4]_2 \cdot EtOH$ (0.5 mmol), in ethanol (100 cm^3) at 50—60 °C, was added $Cu(ClO_4)_2 \cdot 6H_2O$ (1.2 mmol). After stirring for *ca.* 1 h, the green suspension of the product was filtered off and washed with ethanol. Yield 60—70%.

$[Cu_2L(MeCN)_2][ClO_4]_2$ ($L = L^1$ *or* L^2). To a solution of the Group 2 perchlorate complex, $[ML][ClO_4]_2$ (5 mmol), dissolved in MeCN–EtOH (50—25 cm^3) under argon was added $[Cu(MeCN)_4]ClO_4$ (10 mmol). The yellow product crystallised in good yield ($L = L^1$, 80%; L^2, 82%).

$[Cu_2L(pydz)_2][ClO_4]_2$ ($L = L^1$ *or* L^2). $[Cu_2L(MeCN)_2][ClO_4]_2$ (0.05 mmol) was dissolved in dry deoxygenated acetonitrile (4 cm^3) and excess pyridazine (0.25 mol) added dropwise under N_2. The solution was heated for *ca.* 10 min and orange-red crystals of the product were obtained on standing. Yield: $L = L^1$, 75%; L^2, 64%.

$[Cu_2L(cis\text{-}Ph_2N_2)_x(MeCN)_y][ClO_4]_2$ ($L = L^1$, $x = 2$, $y = 0$: $L = L^2$, $x = 1$, $y = 1$). $[Cu_2L(MeCN)][ClO_4]_2$ (0.06 mmol) was dissolved in deoxygenated acetonitrile (5 cm^3) with gentle heating. To this solution was added under N_2, *cis*-azobenzene (0.15 mmol) dissolved in deoxygenated ethanol (6 cm^3). A deep red colour developed on addition which darkened with heating. On leaving to cool under N_2, black crystals of the product were isolated. Yield: $L = L^1$, 58%; L^2, 68%.

Table 5. Atomic co-ordinates ($\times 10^4$) with estimated standard deviations in parentheses for $[Cu_2L^2(pydz)_2][ClO_4]_2$

Atom	*x*	*y*	*z*
Cu	113(2)	975(1)	322(2)
N(1)	1 870(14)	1 676(8)	394(11)
C(2)	1 961(19)	2 480(10)	1 056(16)
C(3)	521(20)	2 965(10)	913(16)
C(4)	−453(23)	2 544(13)	1 544(19)
N(5)	−988(14)	1 670(9)	1 206(11)
C(6)	−2 015(16)	1 385(14)	1 553(14)
C(7)	−2 721(17)	530(13)	1 292(16)
O(8)	−2 195(11)	−68(7)	693(9)
C(9)	−3 045(20)	−746(10)	630(16)
C(10)	−2 857(20)	−1 529(9)	−26(16)
C(11)	−3 828(24)	255(13)	1 587(17)
C(12)	−4 108(18)	−596(13)	1 184(18)
C(13)	−225(22)	3 115(12)	−294(19)
C(14)	882(23)	3 831(11)	1 443(18)
N(15)	1 095(12)	78(9)	1 556(12)
N(16)	1 246(17)	−716(9)	1 082(13)
C(17)	2 375(19)	−1 204(10)	1 718(15)
C(18)	3 205(17)	−1 016(15)	2 703(13)
C(19)	3 026(21)	−257(15)	3 228(13)
C(20)	1 936(23)	268(12)	2 525(13)
Cl	−4 704(5)	3 194(3)	−989(5)
O(21)	−4 002(18)	3 994(10)	−777(14)
O(22)	−4 730(20)	2 965(12)	−2 068(14)
O(23)	−4 007(13)	2 609(10)	−215(13)
O(24)	−6 104(15)	3 238(10)	−994(15)

Physical Measurements.—Oxygen uptake measurements were carried out as described in an earlier paper.[11] Infrared spectra were measured as KBr discs and Nujol mulls using a Perkin-Elmer 598 spectrometer. ^1H N.m.r. spectra were recorded at 250 MHz using a Bruker WM250 instrument. Electronic spectra were obtained with a Perkin-Elmer λ9 spectrophotometer.

X-*Ray Structure Determination of* $[Cu_2L^2(pydz)_2][ClO_4]_2$.—*Crystal data.* $C_{30}H_{36}Cl_2Cu_2N_8O_{10}$, $M = 866.7$, monoclinic, space group $P2_1/c$, $a = 9.71(1)$, $b = 15.64(2)$, $c = 12.52(1)$ Å, $\beta = 105.5(1)°$, $U = 1\,832.6$ Å^3 (cell dimensions obtained by measurement of 20 high-angle axial reflections), $D_m = 1.55(3)$, $D_c = 1.57$ g cm^{-3}, $F(000) = 888$, $\lambda = 0.7107$ Å, $\mu = 23.8$ cm^{-1}.

Precession photographs established the preliminary cell constants and space group. A crystal (0.25 × 0.20 × 0.35 mm) was mounted to rotate around the *a* axis on a Stoe STADI2 diffractometer and data were collected *via* a variable width ω scan. Background counts were 20 s and a scan rate of 0.033° s^{-1} was applied to a width of $(1.5 + \sin\mu/\tan\theta)$. 3 101 Independent reflections with $2\theta < 50°$ were measured of which 1 154 having $I > 1.5\sigma(I)$ were used in the subsequent refinement. The structure was solved from the Patterson function. The cation contained a crystallographic centre of symmetry. All non-hydrogen atoms were refined anisotropically. Hydrogen atoms were fixed in trigonal or tetrahedral postions but those bonded to the same carbon atom were given a common refined thermal parameter. The structure was refined using full-matrix least squares to *R* 0.075 (*R′* 0.086).

Table 6. Molecular dimensions in the co-ordination sphere* of $[Cu_2L^2(pydz)_2][ClO_4]_2$; distances in Å, angles in °

Cu–N(1)	2.010(13)
Cu–N(5)	2.044(11)
Cu–N(15)	2.116(14)
Cu–N(16′)	1.938(14)
N(1)–Cu–N(5)	104.3(5)
N(1)–Cu–N(15)	96.7(5)
N(5)–Cu–N(15)	99.0(5)
N(1)–Cu–N(16′)	121.2(6)
N(5)–Cu–N(16′)	106.0(6)
N(15)–Cu–N(16′)	126.0(5)

* Primes denote symmetry element $-x, -y, -z$.

The weighting scheme used was $w = 1/[\sigma^2(F) + 0.003F^2]$ where $\sigma(F)$ was taken from counting statistics. This gave equivalent values of $w\Delta^2$ over ranges of F_o and $\sin\theta/\lambda$. In the final cycle of refinement no shift/error was >0.1 and the final difference Fourier showed no significant peaks. Calculations were performed using SHELX 76[12] and local programs on the Amdahl V7/A computer at the University of Reading. Final co-ordinates are given in Table 5 and the geometry of the co-ordination sphere in Table 6.

Acknowledgements

We thank the Department of Education, Northern Ireland, and the S.E.R.C. for support. Acknowledgement is also due to the S.E.R.C. for a studentship (to P. C. Y.), and for funds for the diffractometer and the Perkin-Elmer λ9 u.v.–visible spectrometer. We also thank Mr. A. W. Johans for help with the crystallographic investigations.

References

1 M. G. B. Drew, F. S. Esho, and S. M. Nelson, *Inorg. Chim. Acta*, 1983, **76**, L269; M. G. B. Drew, F. S. Esho, A. Lavery, and S. M. Nelson, *J. Chem. Soc., Dalton Trans.*, 1984, 545.
2 S. M. Nelson, F. S. Esho, and M. G. B. Drew, *J. Chem. Soc., Chem. Commun.*, 1981, 388.
3 M. G. B. Drew, A. Lavery, F. S. Esho, and S. M. Nelson, *J. Am. Chem. Soc.*, 1983, **105**, 5698.
4 S. M. Nelson, J. T. Grimshaw, A. Lavery, K. McKillop, and M. G. B. Drew, 'Substrate Binding and Dioxygen Activation at diCopper Sites,' in 'Biological and Inorganic Copper Chemistry,' eds. K. Karlin and J. Zubieta, Adenine, New York, 1985, pp. 35—40.
5 D. T. Cromer and A. C. Pearson, *Acta Crystallogr., Sect. B*, 1972, **28**, 1052.
6 M. G. B. Drew and P. C. Yates, *J. Chem. Soc., Dalton Trans.*, 1987, 2563.
7 A. Lavery, Ph.D. Thesis, Queen's University, Belfast, 1984.
8 P. Rademacher, V. M. Bass, and M. Wildemann, *Chem. Ber.*, 1977, **110**, 1939.
9 J. A. Hyatt, *Tetrahedron Lett.*, 1977, 141.
10 M. G. B. Drew, F. S. Esho, and S. M. Nelson, *J. Chem. Soc., Dalton Trans.*, 1983, 1653.
11 S. M. Nelson, A. Lavery, and M. G. B. Drew, *J. Chem. Soc., Dalton Trans.*, 1986, 911.
12 G. M. Sheldrick, SHELX 76, Package for Crystal Structure Determination, University of Cambridge, 1976.

Received 2nd March 1987; *Paper* 7/381